

## A Numerical Study on the Interpretation of Data from Open Atmospheric Balloon Soundings

P. ALEXANDER

*Departamento de Física, Facultad de Ciencias Exactas y Naturales, Universidad de Buenos Aires, Buenos Aires, Argentina*

(Manuscript received 18 February 2004, in final form 24 June 2004)

### ABSTRACT

Wrong information may be extracted from balloon soundings if neither appropriate interpretation and processing nor evaluations of certain inevitable distortions or artifacts on atmospheric measurements are performed. A numerical code that finds solutions to the dynamical and thermal equations describing an open balloon in the atmosphere is used to develop flight simulations under diverse conditions. The results are then employed to point out that a valid determination of values for diverse variables is intrinsically difficult. It is shown that the distance between the balloon and gondola may be chosen to optimize the information to be obtained from observations obtained during ascent and descent, so that even without an accurate balloon-tracking system, it may be possible to reconstruct horizontal wind fluctuations from the measurements. Vertical air oscillations may be only grossly inferred in some cases. The propagation direction of gravity waves detected during a sounding may be inferred and vertical wavelengths may typically be determined with a 10% accuracy. Air velocity measurements performed during flotation may be used to find shears.

### 1. Introduction

In the last few decades a considerable number of soundings have strongly contributed to a better understanding of the lower and middle atmosphere. Data acquisition, by means of rocket-, balloon-, aircraft-, and satellite-borne instrumentation, as well as radar and lidar ground-based methods, virtually constitute the bulk of experimental evidence. Large efforts have been devoted to reduce systematic errors in the measurements. In addition, both with remote sensing and in situ techniques, significant approximations are often required for the calculation of variables or parameters that are not directly observable, which must be carefully evaluated.

The spatial and temporal resolutions of collected data constitute a relevant advantage of balloons. However, many unexpected or foreseen difficulties may be encountered when using these vehicles for soundings. They may deviate from the estimated behavior, the trajectory may be arbitrarily affected by local atmospheric conditions, or diverse, particular approximations may be needed in the calculation of quantities that are indirectly measured. We will refer here to the last aspect.

One of the most fundamental obstacles in the interpretation of wind data is the need for adequate knowledge of the balloon velocity with respect to a fixed frame (the anemometer measures velocities relative to the gondola), particularly in the vertical direction. Another important inconvenience is related to the fact that wave data collected during the ascent or descent provide apparent vertical wavenumbers or intrinsic periods, because the irregular balloon motion and the particular displacement and tilt of the atmospheric modes detected during the sounding cause the measured vertical wavelengths to disagree with the actual instantaneous ones. True vertical wavenumbers could be observed if either there were no horizontal balloon drift and no wave displacement or if the ascent/descent speed were much larger than the vertical phase speed, so that the waves would be seen nearly frozen in space. These ideal situations do not usually occur. Studies of the resulting distortions on measured single waves or spectra have already been performed (Gardner and Gardner 1993; de la Torre and Alexander 1995; Alexander and de la Torre 1999), but they were limited by many simplifications for the atmosphere and balloons in order to obtain analytical results. Another problem associated with balloons is related to the assumption that their horizontal speed follows (and, therefore, measures) the mean wind (see, e.g., Tatom and King 1976), because this may be sometimes doubtful. Furthermore, in the vertical direction a balloon responds to its environment in a complex way. It is a complicated

---

*Corresponding author address:* Dr. P. Alexander, Departamento de Física, Facultad de Ciencias Exactas y Naturales, Universidad de Buenos Aires, Ciudad Universitaria, Buenos Aires 1428, Argentina.  
E-mail: peter@df.uba.ar

combination of factors, because its vertical dynamics is not exclusively related to vertical air motion, but also to buoyancy, the thermal environment, and gravity (Morris 1975). Vertical air motions have been said to be deduced from changes in the ascent rate in some closed (superpressure) balloons (see, e.g., Kitchen and Shutts 1990), but it has been observed that open (zero pressure) balloons may follow density variations, rather than the air vertical motion (de la Torre et al. 1996). Under these conditions it may be wrong to infer air vertical velocity fluctuations from open-balloon ascent rates. In fact, Alexander et al. (1996) employed a simple 1D model, where the analytical solutions for the vertical oscillations of open-balloon during ascent or descent were clearly affected by the vertical wind fluctuations, but even more significantly by the density oscillations when the balloon gas did not thermalize with the surrounding air. In summary, many questions regarding the proper use of balloons and the adequate interpretation of resulting data have arisen.

To make appropriate use of the measurements from soundings performed with open balloons, it is essential to understand the dynamics of these vehicles. This aspect has been analyzed in a previous work (Alexander 2003), with the use of a model implemented in a computational program (Alexander and de la Torre 2003) that removes some limitations of previous studies. Below we perform simulations using the same numerical code. However, our aim here is to analyze the results to provide some further insight into the nature of the problem of properly interpreting data collected on board open balloons, and to improve our present understanding thereof; in particular, we wish to extend some of the earlier works.

## 2. The balloon model and its numerical implementation

A brief description of the balloon model and its implementation in a numerical program is now given. For a detailed description the reader is referred to Alexander and de la Torre (2003). The numerical code obtains solutions for the vertical motions and one horizontal direction. Flights of a few hours, including ascent up to the stratosphere, flotation, and descent, may be studied.

The governing equation for the motion of the balloon stems from the equation for the conservation of momentum of a spherical body coupled with the equation for conservation of the momentum of a fluid. Two alternatives have been implemented for the balloon gas thermal description—either it thermalizes with the surrounding air, or it follows a polytropic evolution with index  $\gamma$ . The polytropic index is related, among many factors, to the balloon skin thermal conductivity (de la Torre et al. 2003). For simplicity, daytime solar heating

and nighttime cooling have not been included in the model. The background air temperature in the height range of 0–32 km and the density at sea level are taken from the *U.S. Standard Atmosphere, 1976*. The dynamic viscosity is constant ( $1.50 \times 10^{-5} \text{ N s m}^{-2}$ ) in the considered altitude interval. The mean flow field profile is taken to be null in the vertical direction, whereas the horizontal component is specified by linear shears in three neighboring height ranges. The perturbations to the mean atmospheric background state have been separated in two ranges—one dominated by the propagation of gravity waves and another that may be parameterized by turbulent viscosity. The dispersion equation and the relations predicted by Hines (1960) between the relative phases and amplitudes of fluctuations of velocity, pressure, temperature, and density for gravity waves were included. Time- and space-dependent bidimensional, monochromatic, sinusoidal gravity waves are employed, and convective saturation may be imposed for them. At the present time no balloon studies seem to have been made that accommodate simultaneous variations of atmospheric density, temperature, and vertical and horizontal velocity components that are due to a gravity wave.

Flight, balloon, and atmosphere characteristics and the numerical requirements must be specified in the input of the numerical code. A null differential velocity between the balloon and atmosphere will be imposed at the start to avoid the appearance of initial transient effects, which are out of the scope of the present work. Saturated waves will be used. An integral term that is present in the equation of motion produces numerical complications, but it is ignored in the code because during typical balloon flights it may be neglected (Tatom and King 1976). In the following section, a systematic study through a variety of numerical simulations and a detailed analysis thereof is given.

## 3. Numerical study

We are interested in a qualitative study of the basic characteristics of some open-balloon data interpretation problems during the ascent from the ground, flotation at some predetermined altitude, and the descent back to the surface. Our analysis will be based on a set of numerical solutions corresponding to a range of typical scenarios (see Alexander 2003). A typical reference case (R) is first considered in an atmosphere with a null background velocity and turbulent viscosity but that includes gravity waves, where the balloon gas thermalizes with the surrounding air. It is possible to constrain within the model the alteration of the primary balloon or atmosphere aspects to four basic independent changes: gas thermodynamics (G), ambient atmospheric velocity (V), air small-scale turbulence (T), and wave characteristics (W). In case G a polytropic gas

evolution is assumed, where  $\gamma = 1.1$ ; in case V a shear for the background atmospheric horizontal velocity is employed; in case T an air turbulent viscosity is introduced; and in case W the horizontal wavelength of the gravity wave is reduced (this leads to a shorter intrinsic period), and its amplitude is increased. Flotation has been set in the five solutions to an altitude about 22 km (lower stratosphere). Horizontal and vertical positions and velocities are respectively designated by  $x, z, u$ , and  $w$  (subindices  $a$  and  $b$  are used to discriminate between air and balloon velocities, respectively), and  $k_z$  indicates vertical wavenumber.

There are peculiarities of each flight that may influence the observations in a different way. This could reveal that the necessary data interpretation depends on the characteristics of each case. Let us first analyze the horizontal wind measurements. To find the air horizontal velocity from the relative value  $u_a - u_b$  measured on board, we will need a precise tracking of the system. However, this is not always possible, and so we must look for adequate alternatives. In Fig. 1 we may compare the horizontal air velocity as seen from the balloon and from the ground. Notice that the balloon horizontal motion does not respond exactly to the wind fluctuations, which act with the mean speed as forcing functions, and so it exhibits some significant and predictable deviations. In fact, balloons follow closely the local wind in the horizontal direction, and open balloons will exhibit a short delay and slightly smaller amplitude in their response (Alexander 2003). Then, we may write during ascent and descent a kind of Lagrangian description in terms of time  $t$ ,  $u_a \approx A \sin[\Omega(t - t_0)]$  and  $u_b \approx A \sin[\Omega(t - t_0) - \varphi]$ , and so

$$u_a - u_b \approx \varphi A \sin[\Omega(t - t_0) + 90^\circ], \tag{1}$$

where  $t_0$  is an adequately chosen time,  $A$  is the amplitude,  $\Omega$  is the apparent wave frequency as seen from the balloon, and (we define for use below)  $\Omega t_* = 90^\circ$ . As expected, the difference between the two slightly shifted sinusoidal curves is  $90^\circ$  out of phase with them. The amplitude of the relative velocity is typically 0.2A in Fig. 1, and so the phase shift  $\varphi \approx 0.2$ . From Eq. (1) we see that we need to know the typical phase shift in order to be able to adequately find the air horizontal velocity from the measurements, because

$$u_a(t + t_*) = (u_a - u_b)(t)/\varphi. \tag{2}$$

However, the gondola with the measuring devices is usually a large distance under the balloon. In an atmosphere where the shear of the horizontal velocity due to the wave is much larger than the mesoscale gradient, an anemometer in a gondola located at a distance  $h$  under the balloon (with  $hk_z/2\pi \ll 1$ ) provides very indirect measurements of the quantity we wish to find as

$$u_{ah} - u_b = u_{ah} - u_a + u_a - u_b \approx \frac{\partial u_a^E}{\partial z}(-h) + \varphi u_a|_{t+t_*}, \tag{3}$$

where superscript  $E$  refers to the Eulerian point of view and subscript  $h$  refers to that distance under the balloon. To evaluate the derivative during ascent or descent we take into account that during these stages the evolution of the wave phase at the balloon position  $\phi_b$  is essentially given by the change in the vertical position (the effect of wave displacement and balloon horizontal motion is negligible), and so

$$u_a = A' \sin[-k_z(z - z_o)].$$

The balloon phase progression will match the Lagrangian description [ $\Omega(t - t_0)$  is a positive and increasing expression, and we take  $k_z > 0$ ] only if we define  $A' = -A$  and  $A' = A$  respectively for ascent and descent. In addition,

$$\begin{aligned} u_{ah} - u_a &= A' \sin\{-k_z[(z - z_o) - h]\} \\ &\quad - A' \sin[-k_z(z - z_o)] \\ &\approx k_z h A' \cos[-k_z(z - z_o)] \\ &= -k_z h A' \sin[k_z(z - z_o) - 90^\circ], \end{aligned}$$

and so the measurements from the gondola are

$$u_{ah} - u_b \approx hk_z u_a|_{t \pm t_*} + \varphi u_a|_{t+t_*}, \tag{4}$$

where plus (minus) in  $\pm$  corresponds to the situations where  $\phi_b$  tends to increase (decrease) during the particular stage [the former (latter) will apply when the balloon with respect to the wave field and the wave field itself are moving with the opposite (same) vertical sense]. In our simulations the typical ascent and descent rates are about  $5 \text{ m s}^{-1}$ , and the tilted wave fronts move upward ( $k_z > 0$ ) with a speed that is about an order of magnitude smaller.

The measurements of horizontal velocity from the gondola reflect two combined effects [see Eq. (3)]—the gradient that is due to the distance between balloon and measuring position and the short delay of the balloon with respect to the air. To extract confident information from the observations it would be convenient to choose  $h$  so that one term dominates the other. However, to ensure this condition we would need to approximately know in advance what kind of wavelengths will be found during the flight, which may be possible only for some soundings. If  $h \ll \varphi/k_z$ , then Eq. (2) may be straightforwardly applied to find out the air horizontal velocity. If  $h \gg \varphi/k_z$ , we must still ensure that  $hk_z/2\pi \ll 1$  (see above) in order to be then able to obtain  $\partial u_a^E/\partial z$  from the flight data. If, in addition, we can measure  $k_z$  during the sounding (see below), we may find the proportionality constant that links our measurements at  $t$  with the air horizontal velocity at  $t + t_*$  [we will be

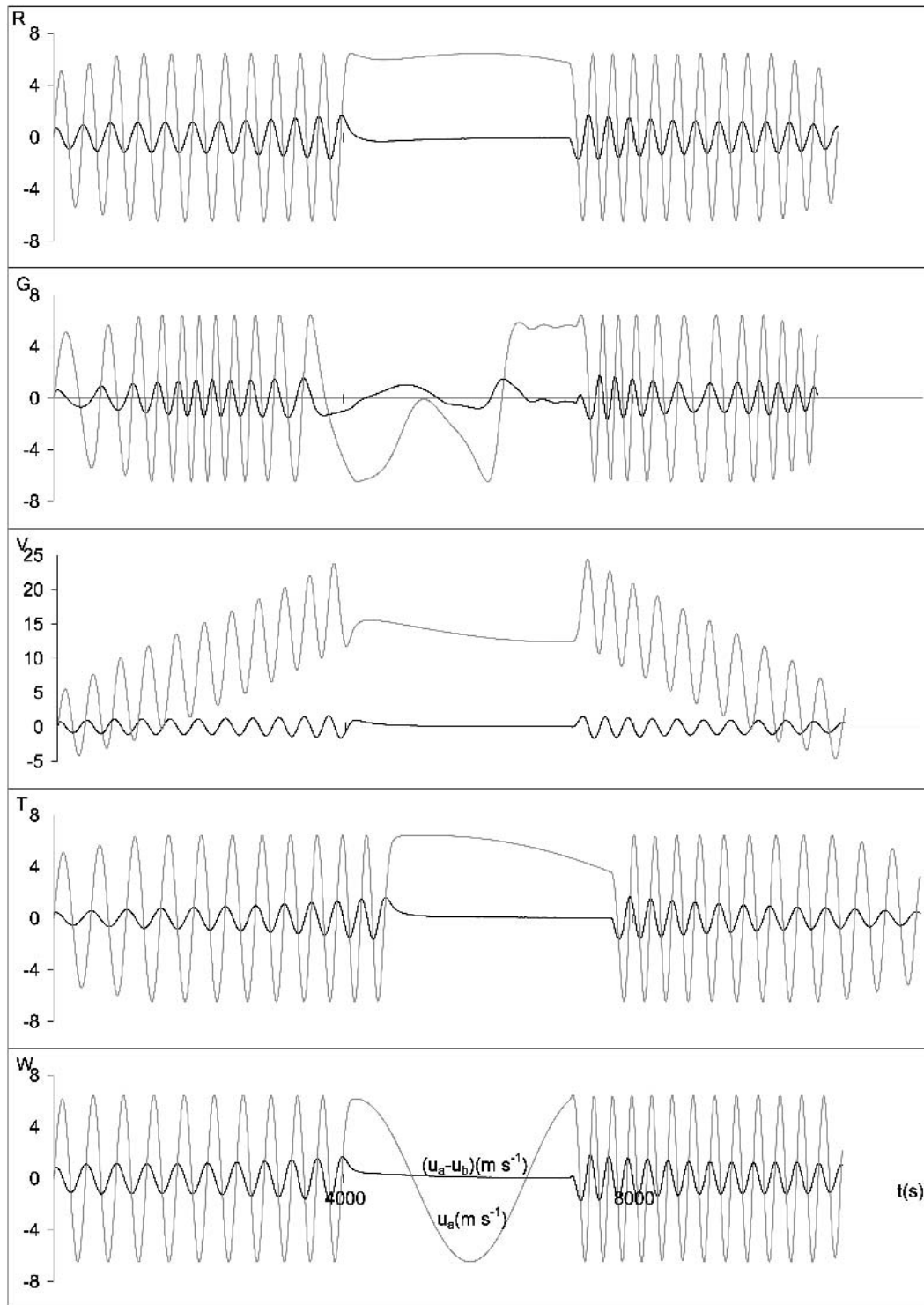


FIG. 1. Air horizontal velocity at the current balloon position as seen from the ground (gray curve) and as observed relative to this vehicle (black curve) during ascent, flotation, and descent.

probably more interested in replacing time by the corresponding height to obtain  $u_a(z)$ ].

In Fig. 2 we show for the five cases the air horizontal velocity 200 m under the balloon and the values relative

to the gondola that would be detected by an anemometer. Here,  $hk_z \approx 0.6$  and  $\varphi \approx 0.2$ , and so the first term on the right-hand side in Eq. (4) is more relevant than the second one, but the latter is not negligible. Both are,

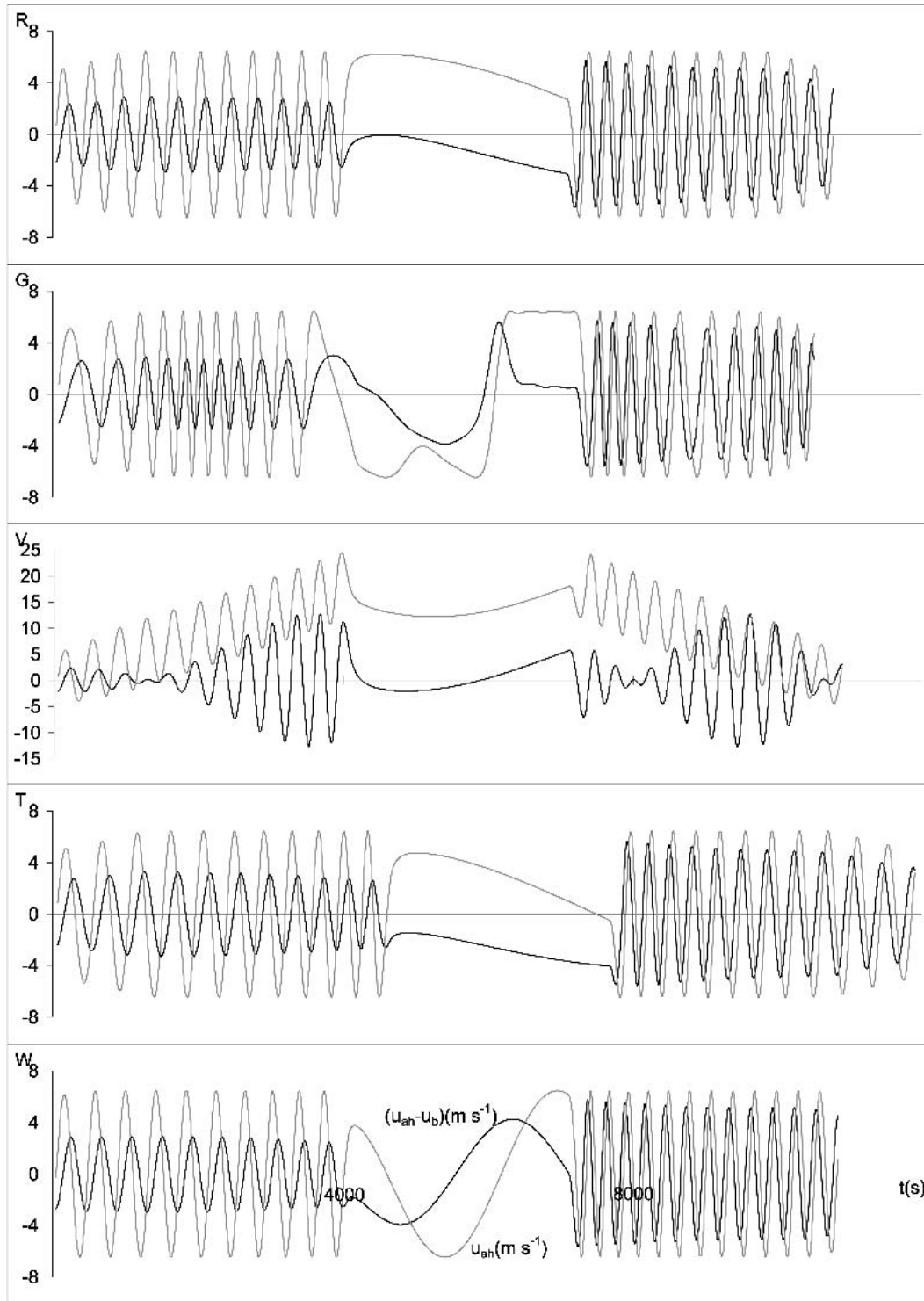


FIG. 2. Air horizontal velocity at the current gondola position as seen from the ground (gray curve) and as observed from an anemometer on board (black curve) during ascent, flotation, and descent.

respectively, out of and in phase during ascent and descent. In our simulations,  $\phi_b$  decreases (increases) during balloon ascent (descent) (the wave fronts move slowly upward); then, in the first term on the right-hand

side  $- (+)$  applies during the former (latter) stage in the five runs. Comparing with Fig. 1, we may see that the prevalence of the term with  $h$  has modified the phase difference between the measurement of the hori-

zonal velocity and its actual value during the ascents. However, the second term on the right-hand side in Eq. (4) reduces (increases) the amplitude of the detected waves during ascent (descent). This gives us some additional information with respect to the relative motion of the waves and balloon during each stage of the sounding. When the balloon descends it is found that both terms in Eq. (4) are not opposite, but are in phase. Corresponding arguments would apply for simulations with the wave fronts moving downward. Then, it will be possible, according to the measured amplitudes of  $u_{ah} - u_a$ , to infer the vertical propagation sense if the wave does not suffer significant alterations during the sounding (notice, in fact, in agreement with the above values for  $hk_z$  and  $\varphi$ , that the amplitude of the differential velocity in all graphs in Fig. 2 is roughly 0.4 and 0.8 times the air horizontal velocity, respectively, for waves in the same or opposite balloon motion, except in case V, which will be explained below). If the vertical phase speed was similar to the ascent or descent rate it would be possible to detect this fact from the apparent vertical wavelengths (they will be much shorter when the wave and balloon are in opposition).

In Fig. 2  $u_{ah}$  looks very similar to  $u_a$  in Fig. 1 because it is the measurement of the same variable 200 m below, which is not very significant in terms of the typical variation scales of the atmospheric variables. We have seen above that  $u_{ah} - u_a$  may be set proportional to  $u_a$ , where the constant may be calculated. Notice that the mesoscale horizontal wind shear is nonzero only in case V, but it is roughly much smaller than the vertical gradient induced by the wave (respectively,  $8 \times 10^{-4} \text{ s}^{-1}$  and  $3 \times 10^{-3} \text{ s}^{-1}$ ). If the opposite would hold we have to replace the first term of Eq. (4) by the Eulerian horizontal wind shear, and we would not be able to obtain  $u_a$  directly from the data. In addition, this case shows the consequences of excessive idealization of the situation. If there is a background wind shear the wave will stretch, because the horizontal speed of the intrinsic system varies with height. The relation between  $u_a$  and  $u_{ah}$  will not be just a small phase shift due to the difference in altitude, and  $u_{ah} - u_b$  in Fig. 2c will be dominated by the changing shear of  $u_a$  between the two heights, so it will exhibit the minimum (maximum) amplitude when  $u_a$  and  $u_{ah}$  peaks coincide (oppose). This completely eliminates the effect on the amplitude described above to infer wave propagation direction (notice also the particular scale of this graph).

Let us now study the vertical wind measurements. Open-balloon response in the vertical direction has been studied by Alexander (2003). It was found that its fluctuations mimic the corresponding component of the air oscillations when the gas thermalizes with the surroundings; but, under a polytropic evolution, they are rather driven by the air density variations. Even the small discrepancies between balloon and air vertical fluctuations under the thermalization condition deserve

some discussion because of their consequences on the measurements of the air vertical velocity. In some parts (particularly in case G) the balloon even leads the air vertical motion. This happens because it is also driven by density changes, not only by air vertical velocity oscillations [density peaks lag (lead) by  $90^\circ$  the vertical velocity maxima due to decreasing (increasing)  $\phi_b$  during ascent (descent)]. In Fig. 3 we may see the balloon vertical velocity fluctuations  $\Delta w_b$  (the mean has been subtracted from the total value), the air velocity ( $w_a \equiv \Delta w_a$ ), and the measured relative value of the latter from the former. With the exception of W, because of the stronger wave, for the ascent and descent in the thermalized cases the balloon vertical velocity lags the air vertical velocity with a short delay in one-half of the cycle; but because of the influence of air density it appears to slightly lead during the remaining half. This shift inversion during the cycle produces the result that the maximum difference (where the original sinusoidal curves are nearly zero) tends to be positive (negative) during ascent (descent). Similar to the horizontal velocity analysis, positive/negative allows the determination of the relative motion of wave field and balloon in cases R, V, and T (Fig. 3), but it will be shown below that this clue becomes masked when measurements are taken from the gondola. In the polytropic case during the ascent and descent  $\Delta w_a \ll \Delta w_b$ , and then essentially  $w_a - \Delta w_b \approx -\Delta w_b$  (no information on  $w_a$  appears in the measurements). In summary, with an accurate balloon tracking we may infer  $w_a$  from  $\Delta w_b$  in the thermalized cases (furthermore during flotation where the average balloon vertical velocity is zero, not shown here), but for the polytropic case  $w_a$  becomes masked by the influence of air density. Moreover, there is a very particular relation between wave and balloon phase and amplitude according to the conditions (the balloon vertical response amplitude exceeds the wave, and peaks of one may lead or lag the other significantly), so it may be hard to establish associations between them in the polytropic case.

In Fig. 4 we plot what would be seen as measured from the gondola 200 m below. This adds now the influence of the gradient of the air vertical velocity to the effect analyzed in the previous figure. We may see that with the exception of case G, because of the alteration introduced by the gradient between the balloon and the gondola, the measurements are not indicative of any variable (the small difference in phase between  $w_a$  and  $w_{ah}$  produces a significant difference between them, which is much larger than  $w_a - \Delta w_b$ ). Because of the particular gradient some peaks become strengthened and others become wiped out or reversed. However, the value of  $w_{ah}$  may still be considered an approximation of  $\Delta w_b$ . In case V we see the same wave-stretching effect as that in Fig. 2. If we determine the vertical wave motion sense (as already shown) and the wavelength (as explained below), we might be indeed able to infer

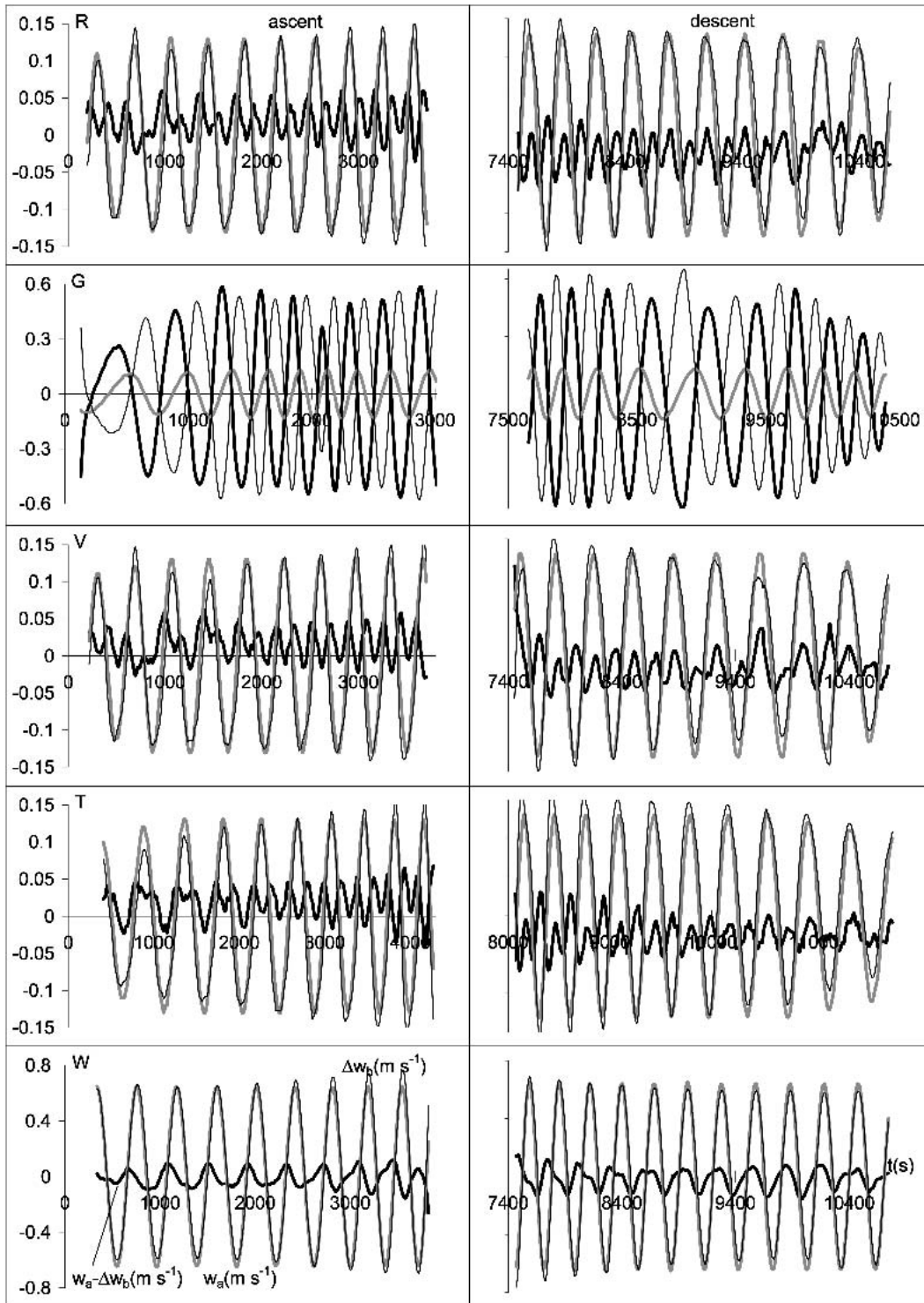


FIG. 3. Air vertical velocity fluctuations at the current balloon position as seen from the ground (thick gray curve) and as observed relative to the vehicle oscillations (thick black curve) during ascent and descent. Balloon fluctuations (thin black curve) are also shown.

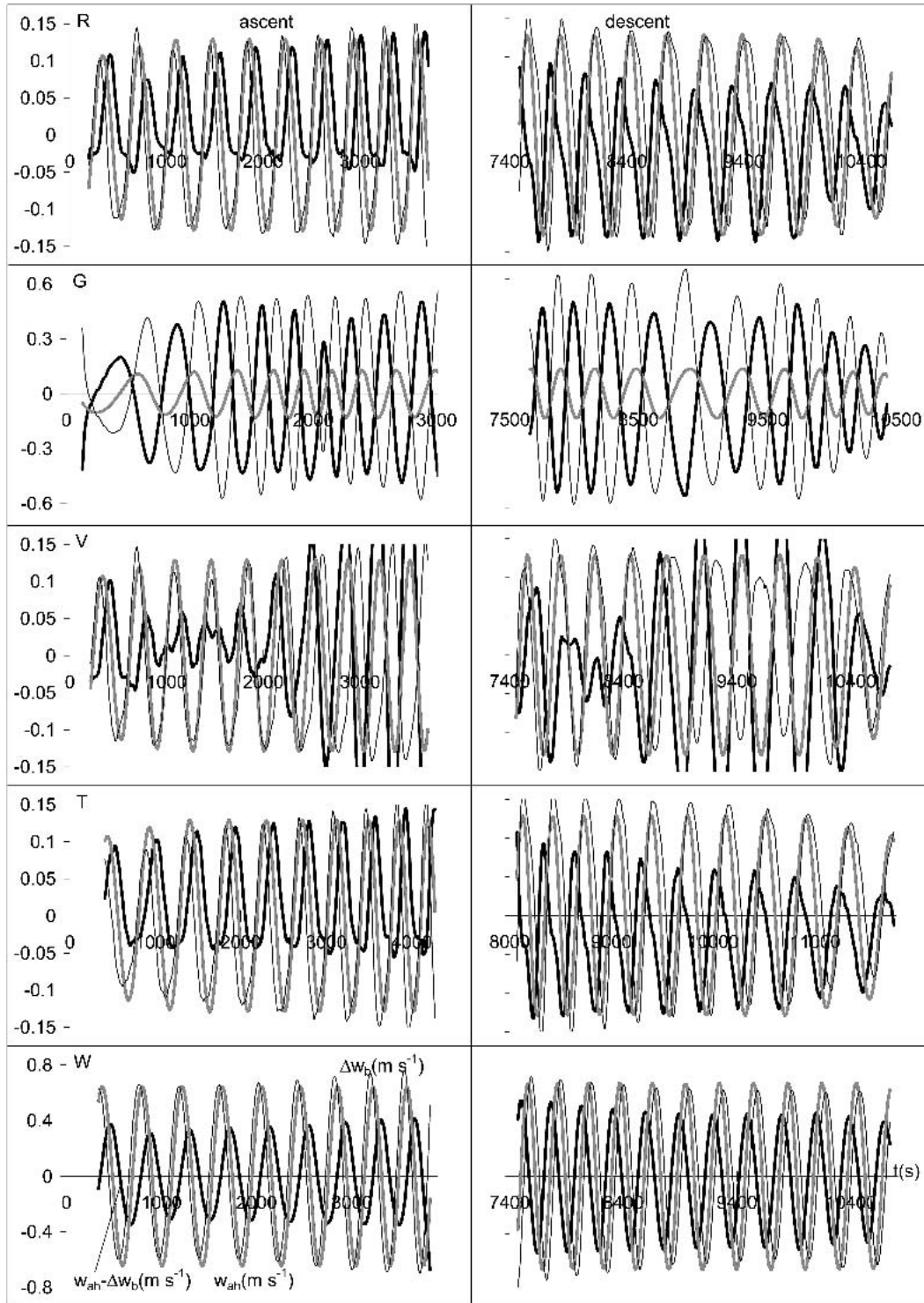


FIG. 4. Air vertical velocity fluctuations at the current gondola position as seen from the ground (thick gray curve) and as observed from an anemometer on board (thick black curve) during ascent and descent. Balloon fluctuations (thin black curve) are also shown.

the air vertical velocity, but accuracy would be a concern.

As we have seen, the measured velocity profiles are not directly and easily linked to the variables of interest, so different precautions have to be considered. If we are interested in measuring vertical wavelengths, we may analyze temperature or density variations to avoid some of the artifacts already discussed in velocity observations, but we will anyway detect apparent values. The vertical wavelength used for the simulations in the five cases is 2 km. After analyzing the air temperature peaks encountered by the balloon during ascent and descent, it was found, on average, that the apparent vertical wavelengths obtained from the observations differ less than 10% in runs R, G, and T and are around this value in cases V and W. The apparent vertical wavelength in V is larger than the true value during the ascent and descent, because of the separation of the wave fronts with time due to the wind gradient, which causes the intrinsic system of the wave to have a different horizontal speed with height. In case W the wave period is shorter than that in the other cases, and it becomes comparable to the ascent and descent time interval. This may be noticed during both stages, which causes the apparent vertical wavelength to become larger (shorter) during the ascent (descent) (according to the relative motion of the wave and balloon). In addition, the slow vertical motion of the gravity waves here considered permits us to take the apparent vertical wavelength that was detected during the ascent and descent as a proxy for the true one, and replacing the value in Eq. (4) finally gives  $u_a$  in terms of the measurements. It should be noted that the vertical motion sense of a wave may be inferred from the comparison of the apparent vertical wavelength that is detected during the ascent and descent if its period and lifetime are of the order of the sounding time.

The present work basically focuses on the interpretation of measurements performed during an open-balloon ascent and descent. During flotation it is not as simple to predict the phase evolution because there is no preponderance of variation due to vertical altitude. It may be seen that during this stage the horizontal balloon motion reproduces the horizontal wind faithfully after an initial transient, regardless of the conditions (see Fig. 1); the same applies in the vertical direction. Then, according to Eq. (3), horizontal velocity data at the gondola position give the velocity shear (Fig. 2). Regarding the vertical data, according to Alexander (2003), the balloon motion changes significantly if flotation time is comparable to the wave period, which only occurs for case W. Because in addition air fluctuations are more significant in this case, we notice that during flotation  $w_b$  tends to equal  $w_a$ , so the measurements may be used to infer the air vertical velocity shear. However, in the remaining four cases there are only tiny effects, which would be masked by any other phenomenon in real soundings.

#### 4. Conclusions

Direct observation of the required variables is seldom performed during balloon soundings. Diverse features have to be taken into account to process data as measured from the gondola. Unavoidable distortions, secondary effects, or a lack of information for operational reasons place constraints on the usefulness of the observations. These problems have been evaluated here for diverse vehicle and atmospheric conditions. Balloon ascent and descent were first studied. Options to improve horizontal wind fluctuation calculations from measurements on board in the absence of an accurate balloon tracking system have been presented. It was found that it might be possible to optimize this with an appropriate choice of the distance between the balloon and gondola. Unless the unusual case occurs where wave phases overtake the balloon during ascent or descent, a different wave velocity amplitude detected during both stages allows us to infer whether they are moving up or downward. The air vertical velocity cannot be accurately inferred from the measurements, but if the gas thermalizes with the surroundings then the balloon vertical fluctuations in any stage may be taken as indicative of that quantity. The observed vertical wavelengths may typically differ by about 10% from the true ones. Air velocity measurements obtained during flotation may be used to infer shears.

There are surely many more flight circumstances than those here described, we just show some examples of necessary procedures that should be considered and that could be easily or more arduously extended to other cases.

*Acknowledgments.* The author is a member of Conicet. This work was supported by grant Ubacyt X021.

#### REFERENCES

- Alexander, P., 2003: A numerical study of open atmospheric balloon dynamics. *Phys. Fluids*, **15**, 3065–3078.
- , and A. de la Torre, 1999: The interpretation of saturated spectra as obtained from atmospheric balloon measurements. *J. Appl. Meteor.*, **38**, 334–342.
- , and —, 2003: A program for the simulation and analysis of open atmospheric balloon soundings. *Comput. Phys. Commun.*, **151**, 96–120.
- , J. Cornejo, and A. de la Torre, 1996: The response of an open stratospheric balloon in the presence of inertio-gravity waves. *J. Appl. Meteor.*, **35**, 60–68.
- de la Torre, A., and P. Alexander, 1995: The interpretation of wavelengths and periods as measured from atmospheric balloons. *J. Appl. Meteor.*, **34**, 2747–2754.
- , H. Teitelbaum, and F. Vial, 1996: Stratospheric and tropospheric gravity wave measurements near the Andes Mountains. *J. Atmos. Terr. Phys.*, **58**, 521–530.
- , P. Alexander, and J. Cornejo, 2003: A relationship between

- skin thermal conductivity and gas polytropic index in an open atmospheric balloon. *J. Appl. Meteor.*, **42**, 325–330.
- Gardner, C. S., and N. F. Gardner, 1993: Measurement distortion in aircraft, space shuttle, and balloon observations of atmospheric density and temperature perturbation spectra. *J. Geophys. Res.*, **98**, 1023–1033.
- Hines, C. O., 1960: Internal atmospheric gravity waves at ionospheric heights. *Can. J. Phys.*, **38**, 1441–1481.
- Kitchen, M., and G. J. Shutts, 1990: Radiosonde observations of large-amplitude gravity waves in the lower and middle stratosphere. *J. Geophys. Res.*, **95**, 20 451–20 455.
- Morris, A. L., 1975: Scientific ballooning handbook. NCAR Tech. Note TN-99+IA, 478 pp.
- Tatom, F. B., and R. L. King, 1976: Determination of constant-volume balloon capabilities for aeronautical research. NASA Contractor Rep. CR-2805, 169 pp.